Membrane Water Treatment, Vol. 1, No. 3 (2010) 215-230
DOI: http://dx.doi.org/10.12989/mwt.2010.1.3.215

Water desalination by membrane distillation using PVDF-HFP hollow fiber membranes

M.C. García-Payo[1], M. Essalhi[1], M. Khayet[1]*, L. García-Fernández[1], K. Charfi[1] and H. Arafat[2]

[1]*Department of Applied Physics I, Faculty of Physics, University Complutense of Madrid, Av. Complutense s/n, 28040, Madrid, Spain*
[2]*Department of Chemical Engineering, Faculty of Engineering, An-Najah National University, P.O. Box 7, Nablus, Palestine*

(Received July 10, 2009, Accepted June 14, 2010)

Abstract. Poly(vinylidene fluoride-*co*-hexafluoropropylene), PVDF-HFP, hollow fiber membranes were prepared by the dry/wet spinning technique using different polyethylene glycol (PEG) concentrations as non-solvent additive in the dope solution. Two different PEG concentrations (3 and 5 wt.%). The morphology and structural characteristics of the hollow fiber membranes were studied by means of optical microscopy, scanning electron microscopy, atomic force microscopy (AFM) and void volume fraction. The experimental permeate flux and the salt (NaCl) rejection factor were determined using direct contact membrane distillation (DCMD) process. An increase of the PEG content in the spinning solution resulted in a faster coagulation of the PVDF-HFP copolymer and a transition of the cross-section internal layer structure from a *sponge-type* structure to a *finger-type* structure. Pore size, nodule size and roughness parameters of both the internal and external hollow fiber surfaces were determined by AFM. It was observed that both the pore size and roughness of the internal surface of the hollow fibers enhanced with increasing the PEG concentration, whereas no change was observed at the outer surface. The void volume fraction increased with the increase of the PEG content in the spinning solution resulting in a higher DCMD flux and a smaller salt rejection factor.

Keywords: water treatment; poly(vinylidene fluoride-*co*-hexafluoropropylene); hollow fiber; membrane distillation.

1. Introduction

Membrane distillation (MD) is one of the non-isothermal separation processes using micro-porous hydrophobic membranes. The MD driving force is supplied by the vapour pressure difference resulting from either a temperature difference between both membrane sides or by applying vacuum in the permeate side (El-Bourawi *et al*. 2006, Khayet 2008). Most of the MD applications have been the concentration of several non-volatile solutes in aqueous solutions (salts, sugar, fruit juices, proteins, etc.) (El-Bourawi *et al*. 2006, Gryta *et al*. 2006, Izquierdo-Gil *et al*. 1999, Khayet 2008, Qtaishat *et al*. 2009). In addition, MD process exhibited considerable potential for removal of volatile organic components from water such as chloroform, benzene, different types of alcohols and acids; and also was used effectively for breaking azeotropic mixtures (García-Payo *et al*. 2000 and 2002, Khayet *et al*. 2004).

* Corresponding author, Professor, E-mail: khayetm@fis.ucm.es

Different configurations can be used to carry out the MD process depending on the method followed to establish the driving force (El-Bourawi *et al*. 2006, Qtaishat *et al*. 2008, Khayet 2008). The most used MD configuration is direct membrane distillation (DCMD) because of its simplest design and condensation phenomenon is carried out inside the membrane module. In this case, both the hot feed and the cold permeate liquids are maintained in direct contact with both sides of the membrane (El-Bourawi *et al*. 2006, Khayet 2008). The permeability, long term stability, energy efficiency and rejection factor of the process are highly dependent on the membrane properties (Li and Sirkar 2004, Qtaishat *et al*. 2008, Song *et al*. 2007).

It is well known that a desirable DCMD membrane requires characteristics such as high bulk and surface porosities, optimum pore size and pore size distribution, high degree of pores interconnectivity, high hydrophobicity, low thermal conductivity, anti-fouling characteristics and an optimum thickness in order to provide a high flux, high long term stability and high energy efficiency (Al-Obaidani *et al*. 2008, Martínez and Rodríguez-Maroto 2008).

Commercial hydrophobic membranes prepared for microfiltration and ultrafiltration do not fulfill all the above mentioned characteristics needed for an adequate membrane to be used in DCMD. Subsequently, various research studies have been focused on the fabrication of both flat-sheet and hollow fiber membranes specifically for MD process (Khayet and Matsuura 2001, Park *et al*. 2008, Tomaszewska 1996).

Recently, the copolymer poly(vinylidene fluoride-*co*-hexafluoropropylene) (PVDF-HFP) appeared to be a highly promising material for membrane preparation by non-solvent induced phase inversion (NIPS) technique and was applied in various membrane processes (Cao *et al*. 2006, Feng *et al*. 2006, Li *et al*. 2008, Seol *et al*. 2007, Shi *et al*. 2007 and 2008, Stephan *et al*. 2004, Tian and Jiang 2008, Zhang *et al*. 2008). Compared to poly(vinylidene fluoride) (PVDF) homopolymer, PVDF-HFP presents lower crystallinity and glass transition temperature, and higher solubility and free volume due to the incorporation of an amorphous phase of HFP into the main constituent vinylidene fluoride blocks (Seol *et al*. 2007, Zhang *et al*. 2008). In addition, fluorine content increases due to the addition of hexafluoropropylene (HFP) group, which makes PVDF-HFP more hydrophobic than PVDF. As a consequence, PVDF-HFP is a potential candidate in applications requiring membranes with higher hydrophobicity like MD process.

Most of the studies reported in the literature on PVDF-HFP membrane preparation were conducted using flat-sheet membranes (Cao *et al*. 2007, Feng *et al*. 2006, Li *et al*. 2008, Stephan *et al*. 2004, Tian and Jiang 2008). Nowadays, hollow fiber configuration is one of the most interesting membrane geometry in most separation applications because of its high surface area per unit volume, flexibility in operation, mechanically self-supporting, etc. (Khayet 2003, Khayet *et al*. 2008, Teoh *et al*. 2008). In fact, it is well known that the fabrication of hollow fiber membranes with a desirable performance is not a trivial process because the effects on fiber final morphology, structural characteristics and performance are still not completely clear due to the many interrelating spinning variables involved in the dry/wet spinning technique.

Different structural and morphological types of polymeric hollow fiber membranes have been fabricated by the dry/wet spinning or wet spinning techniques using different dope solutions (polymer type and concentration, additive type and concentration, solvents) as well as different spinning parameters (geometry and dimensions of the spinneret, nature and temperature of the internal and external coagulants, flow rate of the bore fluid, dope extrusion pressure, length and type of the gas gap, wind-up speed, etc.) (Chung 2008). In the literature, PVDF is the most used hydrophobic polymer and has been a subject of active research in polymer science. Several studies have been conducted

to improve the properties of PVDF hollow fiber membranes for MD process (Bonyadi and Chung 2009, Wang *et al*. 1999, Yeow *et al*. 2004). Hou *et al*. (2009) fabricated PVDF/polyethylene glycol (PEG), PVDF/lithium chloride (LiCl) and PVDF/LiCl/PEG hollow fiber membranes for desalination by MD process. It was reported that the presence of PEG favored the formation of thinner fiber skins improving the permeate flux.

Compared to PVDF, research studies using PVDF-HFP hollow fiber fabrication is very scarce. Shi *et al*. (2007, 2008 and 2009) studied the effects of the additives polyvinylpyrrolidone (PVP), LiCl, Tween® 80 (CAS#9005-65-6, Sigma) and glycerol as well as the effects of the air gap distance on the asymmetric structures of PVDF-HFP hollow fiber membranes used as membrane contactors. It was reported that the presence of glycerol in the PVDF-HFP spinning solution resulted in hollow fiber membranes with narrow pore size distribution and the complex of the additives LiCl, Tween^{R} 80 and PVP with glycerol increased the permeate flux of the PVDF-HFP membranes compared to that using a single additive.

In the present study, PVDF-HFP hollow fiber membranes have been prepared by the dry/wet spinning technique using different PEG concentrations and tested for water desalination by DCMD process. The effects of the PEG concentration on the morphological properties of the hollow fiber membranes were studied in terms of scanning electron microscopy (SEM), atomic force microscopy (AFM) and void volume fraction.

2. Experimental

2.1 Materials

Poly(vinylidene fluoride-*co*-hexafluoropropylene) (PVDF-HFP; M_w = 455 kg/mol and M_n = 110 kg/mol). Reagent grade *N,N*-dimethyl acetamide (DMAC) was used as a solvent. Poly(ethylene glycol) (PEG, M_w = 6000) was employed as a non-solvent additive (NSA). Isopropyl alcohol (IPA) was used as a wetting liquid for the measurement of the void volume fraction. Sodium chloride (NaCl) was used to prepare salt aqueous feed solutions in DCMD experiments. All the following chemicals were obtained from Sigma-Aldrich Chemical Co. and used without further purification.

2.2 Preparation of hollow fiber membranes

First, the dope solution was prepared using 19 wt.% PVDF-HFP in a mixture containing the non-solvent additive PEG and the solvent DMAC. PEG was first dissolved in DMAC at room temperature. The PEG concentration in the dope solution was 3 wt.% and 5 wt.%. The balance was DMAC. The dope solution was stirred at 42°C for about 24 h until the copolymer was totally dissolved. Prior to spinning, the dope solution was degassed in an ultrasonic bath for 15 min.

The dry/wet spinning technique was employed for preparation of the hollow fibers as reported elsewhere (García-Payo *et al*. 2009). The spinning conditions are indicated in Table 1. In this study, tap water was used as external coagulant while distilled water was used as internal coagulant (bore liquid). Both the internal and the external coagulants were maintained at 40°C by using a thermostat (Techne, TU-16D). The peristaltic pump (Watson Marlow, 520S) was employed for the circulation of the internal coagulant through the spinneret. The polymer solution was loaded into the spinning dope tank and forced to the spinneret using pressurized nitrogen. After spinning, the fabricated

Table 1 Spinning parameters of PVDF-HFP hollow fiber membranes

Parameter	Operating conditions
Spinneret dimension (OD/ID) (mm)[a]	1.0/0.7
Extrusion pressure (kPa)	50
Bore fluid	Distilled water
Bore fluid flow rate (m^3/s)	$3.2\ 10^{-7}$
External coagulant	Tap water
Bore fluid and external coagulation temperature (°C)	40
Air gap distance (cm)	27.5
Take-up speed (m/s)	0.15

[a]OD and ID refer to outer and inner diameters, respectively

hollow fiber membranes were stored in a water bath at room temperature for at least 24 h to remove the residual solvent DMAC. Subsequently, the hollow fiber membranes were dried in air at room temperature before characterization tests.

2.3 Characterization of hollow fiber membranes

The cross-section of the PVDF-HFP hollow fiber membranes was examined by a field emission scanning electron microscope (FESEM, JEOL Model JSM-6330F). PVDF-HFP hollow fiber samples were fractured in liquid nitrogen and then sputter-coated with a thin layer of gold. The SEM pictures of each hollow fiber membrane sample were taken over different regions of the cross-section.

The inner and outer diameters of the hollow fiber membranes were measured by means of an optical microscope (OLYMPUS BX60M) with a precision of ±1 μm. More than 6 hollow fiber samples and at least 20 measurements were conducted for each sample.

The void volume fraction or porosity of the prepared PVDF-HFP hollow fiber membranes was determined following the method been described elsewhere (Izquierdo-Gil *et al*. 1999, Khayet and Matsuura 2001). In this case three different samples for each hollow fiber membrane were used.

Water entry pressure (LEP_w) of the PVDF-HFP hollow fiber membranes was measured following the method described elsewhere (García-Payo *et al*. 2010). In this case distilled water was pressured from the lumen side of the hollow fiber membranes. From the obtained LEP_w values, the water contact angle was estimated using Laplace-Young equation (García-Payo *et al*. 2002):

$$LEP_w = \frac{-2\gamma_L \cos\theta_w}{r_{max}} \tag{1}$$

where γ_L is the water/vapour tension, θ_w is the water contact angle and r_{max} is the maximum pore radius of the membrane.

Both the internal and external surfaces of the PVDF-HFP hollow fiber membranes were studied by atomic force microscopy (AFM). The images were obtained over different areas of each hollow fiber membrane using Nanoscope III equipped with 1553D scanner (Digital Instruments Inc., Santa Barbara, Ca) in tapping mode. The procedure to take the AFM images has been described elsewhere (Khayet 2003, Khayet and Matsuura 2001, Khayet *et al*. 2008). In the present study, the same tip

was used to scan all hollow fiber surfaces and all captured images were treated in the same way. From the AFM images, the hollow fiber surfaces were characterized in terms of the mean roughness parameter, R_a (minimum, maximum and average values), pore sizes (*i.e.*, mean pore size, geometric standard deviation and pore size distribution) and nodule sizes (*i.e.*, minimum, average and maximum nodule size). The same scan range (*i.e.*, 2×2 μm^2) was considered to evaluate the roughness R_a of each hollow fiber membrane sample in both the internal and external surfaces. The pore size and nodule size are based on the average of at least 60 measurements for each hollow fiber membrane. The cumulative pore and nodule size distributions of both the internal and external surfaces of the PVDF-HFP hollow fiber membranes together with the probability density function curves were obtained following the method described in previous studies (Khayet 2003, Khayet *et al*. 2002).

2.4 DCMD experiments

The PVDF-HFP hollow fiber membranes were tested in DCMD process using distilled water and a salt aqueous solution (NaCl, 30 g/l) as feed. The DCMD experiments were carried out at different feed and permeate temperatures using the experimental set-up described elsewhere (García-Payo *et al*. 2009). Tubular PVDF-HFP hollow fiber membrane modules were first prepared. Eight hollow fiber membranes were cut and packed in a stainless-steel shell-and-tube module using epoxy resin at both ends. In each module the effective length of the hollow fiber membranes was 20 cm.

Both the feed and permeate circulated through the membrane module by means of a double-head peristaltic pump (Watson Marlow, 323). The feed solution was circulated through the lumen side of the membrane module, whereas the permeate solution was circulated through the shell side. The feed and permeate temperatures at the inlets of the membrane module were controlled by means of a heating thermostat (Techne, TU-16A) and a cooling thermostat (Polyscience, 6206), respectively. To measure the temperatures, Pt-100 probes connected to a digital multimeter were installed at both the inlets and outlets of the membrane modules. The membrane module and all tubes were insulated. The permeate flux of each hollow fiber membrane module was determined by weighting the mass in the permeate container as a function of time.

Two series of DCMD experiments were carried out at a constant permeate temperature while the feed temperature was varied. The permeate temperatures were 20 and 25ºC. The effects of the PEG concentration on the permeate flux and the NaCl rejection factor were studied. The rejection factor, R, was calculated as follows:

$$R = \left(1 - \frac{C_p}{C_f}\right) \times 100 \tag{2}$$

where C_p and C_f are the NaCl concentration in the permeate and in the feed solution, respectively. The NaCl concentration was obtained from the electrical conductivity using a conductivimeter (712 Ω Metrohm).

3. Results and discussions

As stated earlier, the cross-section structure of the prepared hollow fiber membranes was characterized by SEM. The obtained images are shown in Fig. 1. The cross-section of the hollow

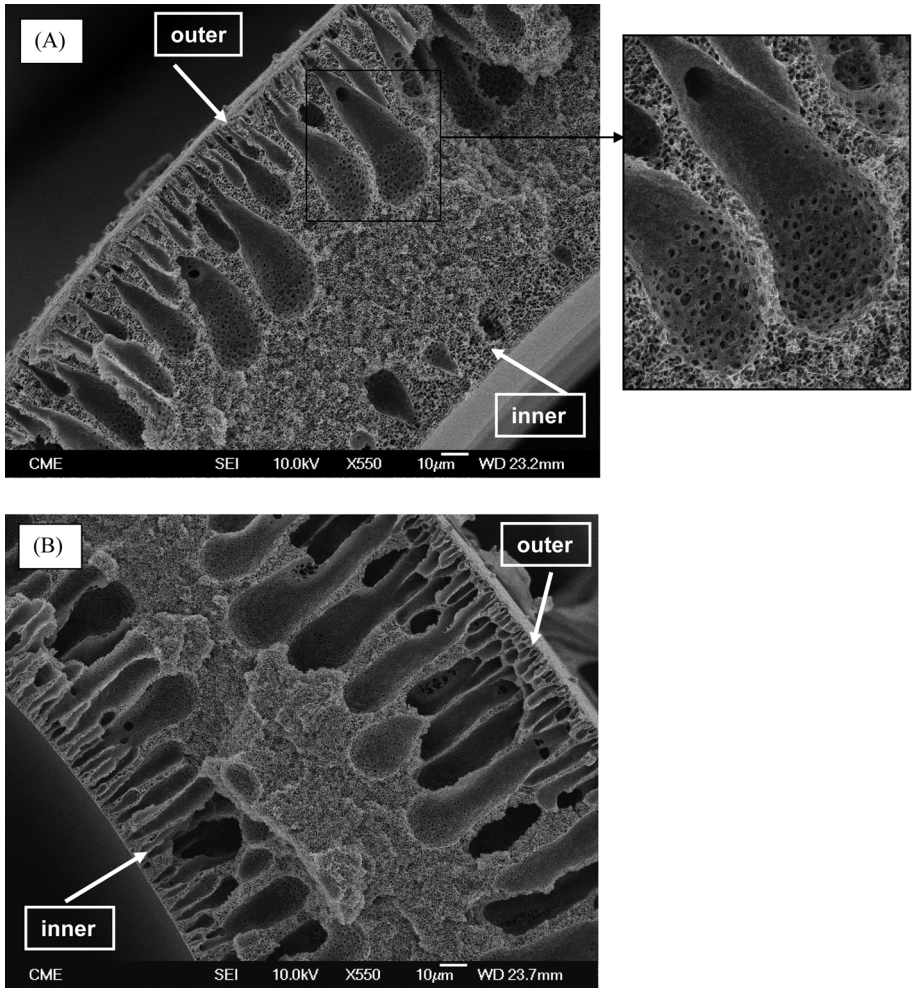

Fig. 1 Cross-section morphology of hollow fiber membranes prepared with different PEG concentrations: (A) 3 wt.%, (B) 5 wt.%

fiber membrane PEG3 exhibits only two layers, an inner sponge-type structure layer and an outer finger-type structure layer, whereas the hollow fiber membrane PEG5 has three layers, one sponge-type structure layer between two finger-type structure layers. As can be seen in Fig. 1(A), the walls of the formed fingers are porous. The number and size of the fingers at the outer layers are smaller for the hollow fiber membrane PEG3. It can also be observed some small voids formed at the internal spongy layer of the hollow fiber membrane PEG3. The number and size of the fingers increase at the inner cross-section of the PVDF-HFP hollow fiber membrane with increasing PEG concentration in the dope solution. Therefore, it can be stated that a high PEG amount in the spinning solution tends to speed up the coagulation rate of the copolymer solution other than forming more porous structure inducing formation of an inner finger-like structure layer (Khulbe *et al*. 2004). It is worth noting that the coagulation of the spun hollow fiber membranes starts from the internal surface and solvent evaporation (*i.e*., DMAC) starts from the outer surface of the nascent

hollow fiber through the air gap distance until reaching the external coagulation bath. In fact, PEG has more affinity to water than the hydrophobic PVDF-HFP. As a result, the diffusion rate of the internal coagulant (*i.e*., water) in the dope solution increases with increasing the PEG concentration. This explains the faster coagulation rate of the copolymer solution and the prompt precipitation inducing more finger-like structure with increasing PEG concentration in the dope solution.

Fig. 2 illustrates the SEM images of the inner and outer surfaces of the PVDF-HFP hollow fiber membranes. As can be seen, an increase of PEG concentration resulted in a more porous inner surface. This effect is less pronounced for the outer surface. Hou *et al*. (2009) observed that the presence of PEG in the spinning solution favoured the formation of thinner skin layers in the spun PVDF hollow fiber membranes. Due to the hydrophilic nature of PEG, an increase of PEG content in the spinning solution increased the precipitation rate, which resulted in the formation of larger fingers like structure that was more pronounced near the inner skin surface because the used air gap length was high. Taking into consideration the above cited results, it is expected higher MD

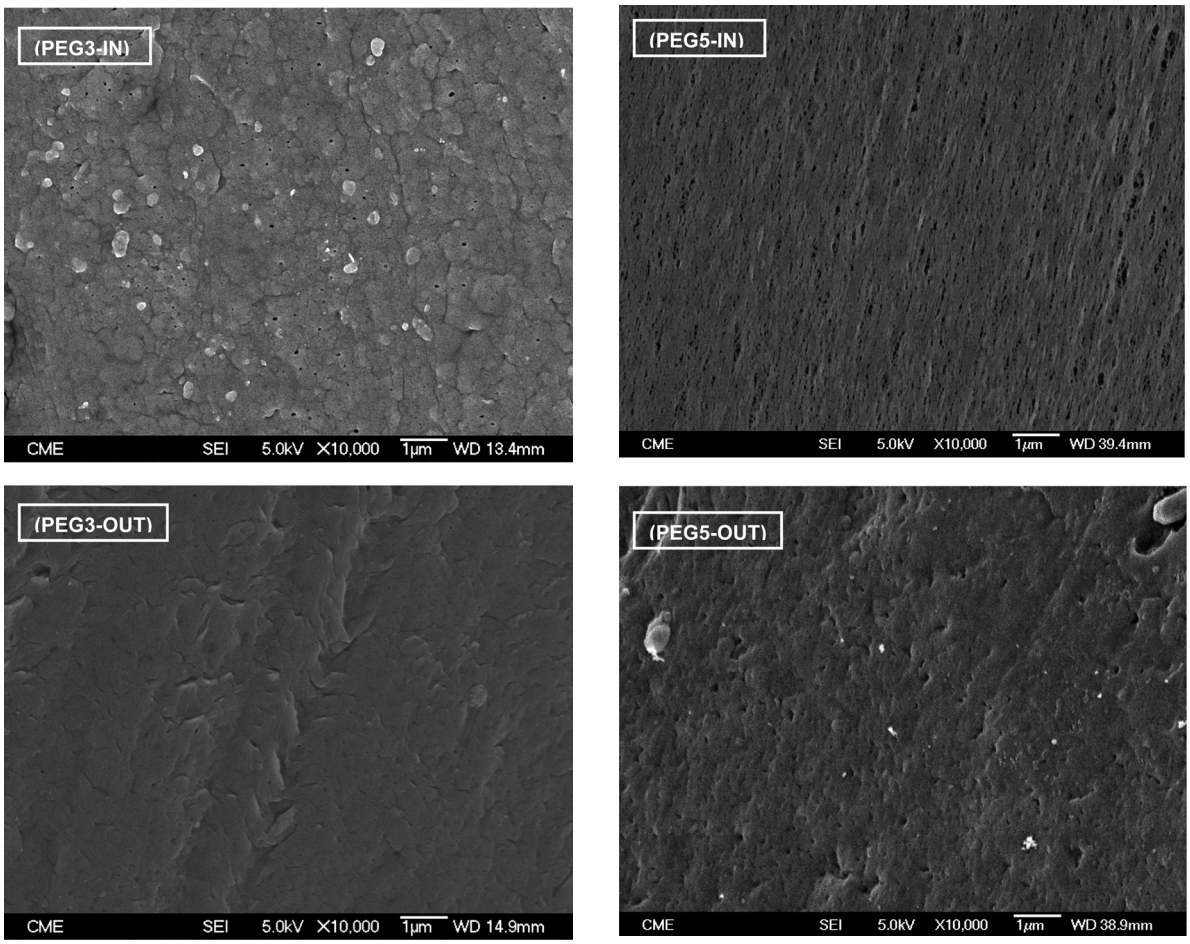

Fig. 2 SEM images of the inner and outer surfaces of the PVDF-HFP hollow fiber membranes prepared with different PEG concentrations

Table 2 Dimensions, void volume fraction, LEP_w and water contact angle of PVDF-HFP hollow fibers prepared at different PEG concentrations

Membrane name	PEG content (wt.%)	Inner diameter (μm)	Outer diameter (μm)	Thickness (μm)	Void volume fraction (-)	LEP_w (10^5 Pa)	Contact angle, θ_w
PEG3	3	1591±52	1716±45	63±34	0.743±0.041	3.6±0.1	76±1
PEG5	5	1315±74	1606±78	145±54	0.807±0.058	3.1±0.2	76±2

permeate flux for the PVDF-HFP hollow fiber membrane PEG5 than for PEG3 hollow fiber membrane.

The internal and external diameters as well as the thickness of the prepared PVDF-HFP hollow fibers are summarized in Table 2. It was found that both the internal and external diameters of the PVDF-HFP hollow fiber membranes decreased with increasing the PEG concentration in the dope solution. A similar behaviour has been reported previously by Park *et al*. (2008) for PVDF hollow fiber membranes and can be attributed to the precipitation rate of the polymer solution. It is worth noting that a reduction of about 17% was observed for the inner diameters between PEG5 and PEG3 membranes, whereas lower reduction (6%) that corresponds to the standard deviations was observed for the outer diameters. It is clear that an increase of the PEG content in the spinning solution affects most significantly the inner structure of the PVDF-HFP hollow fiber membranes due to the fact that the precipitation starts from the internal surface and the PEG has more affinity to water than the copolymer.

It was also observed that the thickness of the PVDF-HFP hollow fiber membrane PEG5 is 2.3 times greater than that of the PVDF-HFP hollow fiber membrane PEG3. This enhancement of the thickness may be attributed to the viscosity of the dope solution, which increased with increasing the PEG concentration in the dope solution inducing an increase of the shear stress of the dope solution within the spinneret. For the considered copolymer solutions, the molecular orientation induced by shear stress within the spinneret is greater at higher PEG concentration and the elongation stress along the spinning line, 27.5 cm, due to the longitudinal force parallel to fiber axis is not high enough to affect the diameters of the PVDF-HFP hollow fiber membrane. In contrast, in this case, the transversal force originated at the exit of the spinneret due to shear stress within the spinneret and swelling is the responsible of PVDF-HFP hollow fiber diameter change affecting more the hollow fiber membrane spun with smaller concentration of the PEG.

The effect of PEG concentration on the void volume fraction of the PVDF-HFP hollow fiber membranes is also presented in Table 2. As it was expected, the void volume fraction is higher for the hollow fiber membrane PEG5. A similar observation has been reported by Hwang *et al*. (2007) for PVDF-HFP flat-sheet membranes fabricated for lithium batteries with different contents of PEG in the copolymer solution. It must be mentioned that, in general, the decrease of the polymer concentration is related with the increase of the non-solvent additive in the dope solution, which may increase the porosity and pore size of the spun hollow fiber membranes (Khayet *et al*. 2002). It is well-known that the void volume fraction (*i.e*., porosity) affects considerably the MD permeate flux. The transmembrane permeate flux is proportional to the porosity. Therefore, it is expected that the MD permeate flux is higher for the PVDF-HFP hollow fiber membrane PEG5. The related results will be presented at the end of this section.

Figs. 3 and 4 show the 3D AFM images of the inner and outer surfaces of the prepared PVDF-HFP hollow fiber membranes, respectively. Significant differences were detected on the inner surfaces

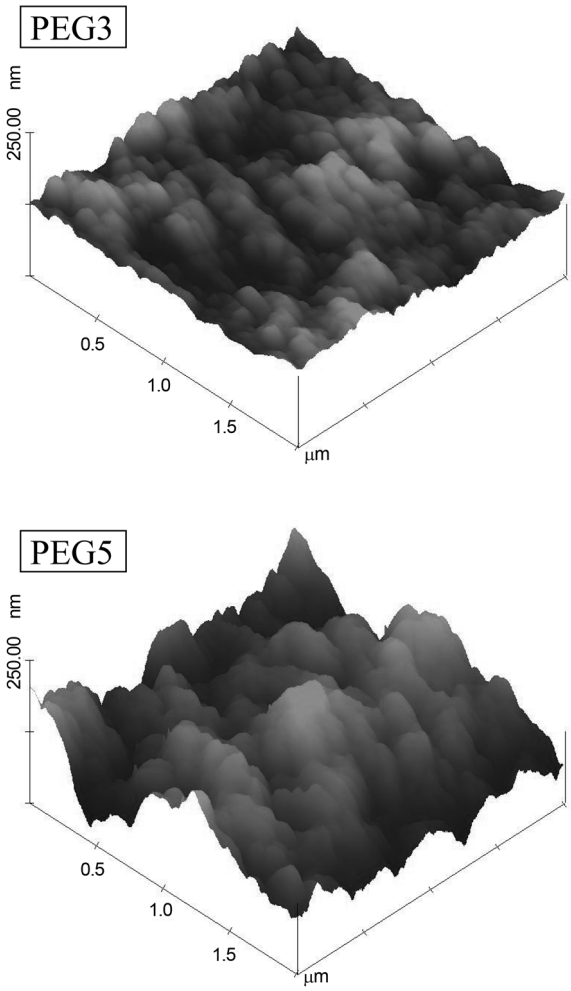

Fig. 3 *3D* AFM images of the inner surfaces of the PVDF-HFP hollow fiber membranes prepared with different PEG concentrations

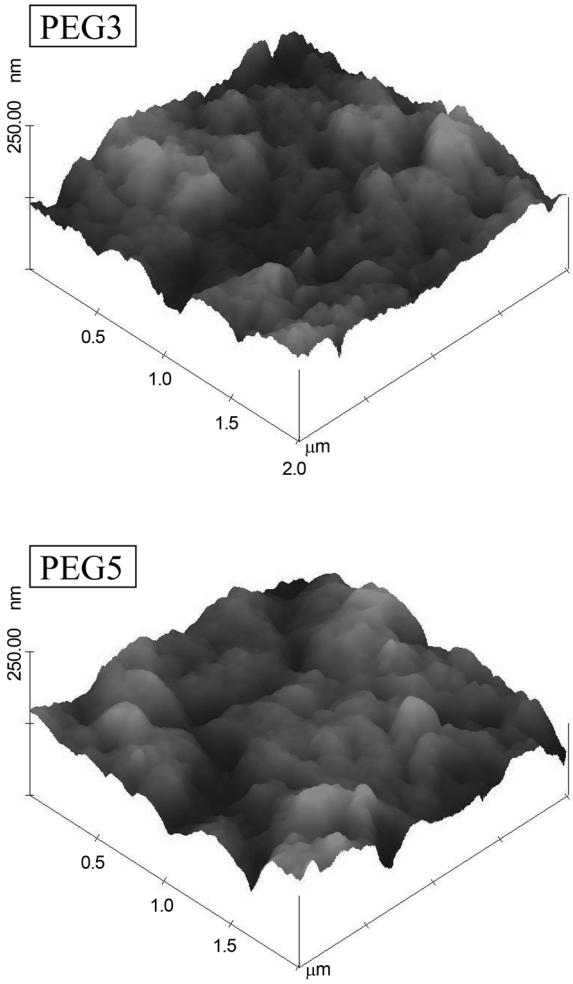

Fig. 4 *3D* AFM images of the outer surfaces of the PVDF-HFP hollow fiber membranes prepared with different PEG concentrations

of the PVDF-HFP hollow fiber membranes prepared with different PEG concentrations. The mean roughness parameter was determined as stated earlier and the minimum, maximum and average values of both the external and internal surfaces of the hollow fiber membranes are summarized in Table 3. An increase of the mean surface roughness of the internal surfaces was observed with increasing the PEG concentration, whereas a quite similar value of the mean surface roughness was determined for the external surface of both hollow fiber membranes PEG3 and PEG5. Moreover, the internal surface of the hollow fiber membrane PEG5 is rougher than its external surface, whereas for the hollow fiber membrane PEG3 the internal surface is smoother than the external surface. These results may be attributed to the viscosity of the dope solution. In fact, the increase of the surface roughness is due to partially to the change of the pore size. It was reported previously that larger pore sizes and higher nodule sizes lead to rougher membrane surfaces (Khayet 2003,

Table 3 Minimum, maximum and average mean roughness parameter, R_a, with the corresponding standard deviation of the internal and external surfaces of PVDF-HFP hollow fibers prepared at different PEG concentrations (scan range considered 2×2 μm^2)

Membrane	R_a (nm) Inside			R_a (nm) Outside		
	Minimum	Maximum	Average	Minimum	Maximum	Average
PEG3	9.6	13.3	11.7±1.2	15.2	33.5	22.9±5.4
PEG5	24.3	52.7	35.4±8.5	13.2	33.2	21.8±5.2

Table 4 AFM mean pore size, μ_p, and geometric standard deviation, σ_p, of the internal and external surfaces of PVDF-HFP hollow fibers prepared at different PEG concentrations

Membrane	Inner surface		Outer surface	
	μ_p (nm)	σ_p	μ_p (nm)	σ_p
PEG3	73.96	1.08	85.72	1.10
PEG5	88.83	1.07	86.01	1.08

Khayet *et al*. 2008, Khulbe *et al*. 2004).

The pore sizes of both the internal and external surfaces of the PVDF-HFP hollow fiber membranes were evaluated and the mean pore sizes together with the corresponding geometric standard deviations were calculated as stated in (Khayet 2003, Khayet *et al*. 2002). The results are summarized in Table 4. The cumulative pore size distributions and the probability density function curves are plotted in Figs. 5 and 6 for the inner and outer surfaces, respectively. The inner surfaces of the hollow fiber membranes exhibit different pore sizes depending on the PEG concentration in the spinning solution. The mean pore size of the inner surfaces increased with the increase of the PEG concentration, whereas no clear change was detected for the mean pore size of the outer surfaces. This may be related with the change of the cross-section structure commented previously, formation of an internal layer containing finger-type structure with increasing PEG concentration in the PVDF-HFP hollow fiber membrane.

The nodule sizes (minimum, maximum, average and standard deviation) are presented in Table 5. The cumulative distribution of nodule size and the corresponding probability density function curves of the internal and external surfaces of each PVDF-HFP hollow fiber membrane are plotted in Figs. 7 and 8, respectively. If the errors intervals are considered, no clear variation can be concluded between the nodule sizes of the internal and external surfaces of PVDF-HFP hollow fiber membranes.

It is known that the liquid entry pressure of water (LEP_w) is related to the hydrophobicity of the membrane as well as to the maximum pore size (García-Payo *et al*. 2002). The measured LEP_w values and the corresponding water contact angle values of the hollow fiber membranes are summarized in Table 2. The considered maximum pore size in Eq. (1) corresponds to the inner surface determined by means of the AFM images as stated earlier. There is a decrease of the LEP_w with the increase of the PEG concentration, whereas no change is observed for the water contact angle. These results may be due to the increase of the membrane pore size with the increase of the PEG concentration in the spinning solution.

Based on the obtained LEP_w values the prepared PVDF-HFP hollow fiber membranes can be used in DCMD. Fig. 9 shows the permeate DCMD flux as a function of different feed temperatures

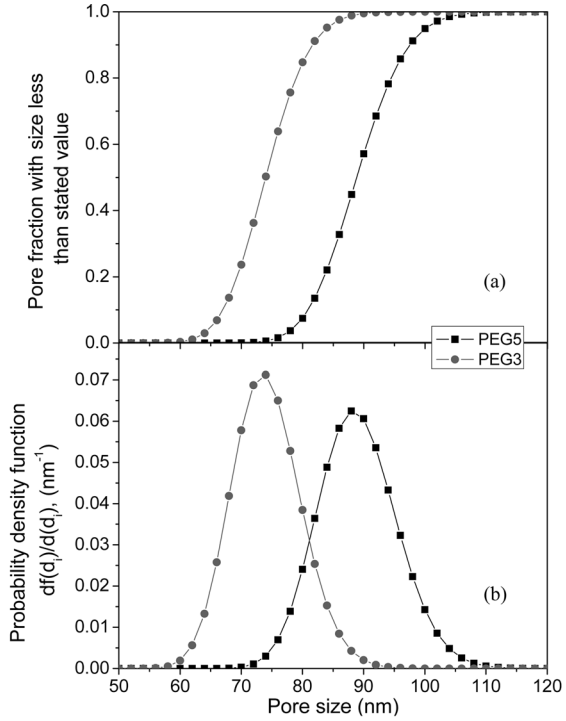

Fig. 5 Cumulative distribution of pore sizes (a) and probability density function (b) curves generated from the pore sizes measured from the AFM images of the inner surfaces of the PVDF-HFP hollow fiber membranes prepared with different PEG concentrations

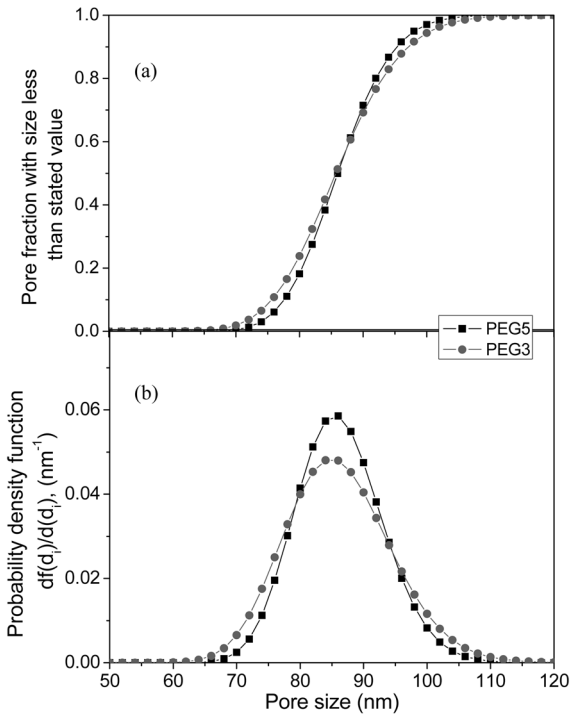

Fig. 6 Cumulative distribution of pore sizes (a) and probability density function (b) curves generated from the pore sizes measured from the AFM images of the outer surfaces of the PVDF-HFP hollow fiber membranes prepared with different PEG concentrations

Table 5 Nodule size (minimum, maximum, average and standard deviation values) of the internal and external surfaces of PVDF-HFP hollow fiber prepared at different PEG concentrations

Membrane	Inner Nodule Size (nm)			Outer Nodule Size (nm)		
	Minimum	Maximum	Average	Minimum	Maximum	Average
PEG3	55	125	93 ± 17	55	161	104 ± 22
PEG5	39	156	97 ± 26	55	125	93 ± 15

maintaining the permeate temperature at 20°C. Distilled water was used as feed. As can be seen, the permeate flux increased exponentially with the feed temperature. It is well-known that in MD process, temperature is the operating variable that affects the MD flux most significantly due to the exponential increase of vapour pressure with temperature (Khayet 2008). Moreover, the DCMD flux increased as the PEG concentration was increased in the spinning solution. This is attributed partially to the porosity, the inner pore size and the roughness. All these parameters increase with the increase of the PEG concentration in the spinning solution. It is worth quoting that the fabricated PVDF-HFP hollow fiber membranes exhibit lower permeate fluxes than those of the PVDF hollow fiber

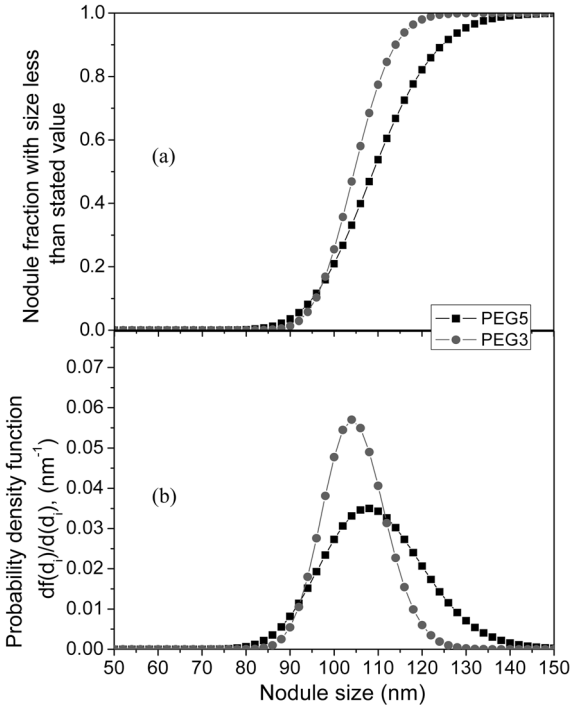

Fig. 7 Cumulative distribution of nodule sizes (a) and probability density function (b) curves generated from the nodule sizes measured from the AFM images of the inner surfaces of the PVDF-HFP hollow fiber membranes prepared with different PEG concentrations

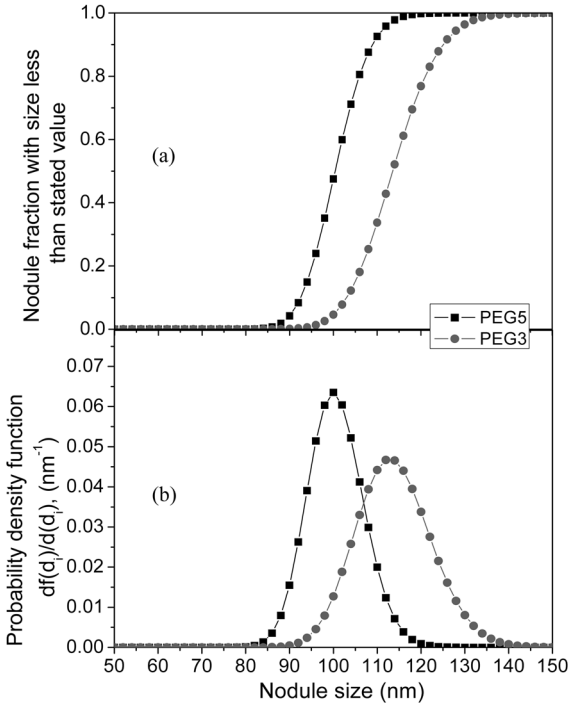

Fig. 8 Cumulative distribution of nodule sizes (a) and probability density function (b) curves generated from the nodule sizes measured from the AFM images of the outer surfaces of the PVDF-HFP hollow fiber membranes prepared with different PEG concentrations

membrane reported by Bonyadi and Chung (2009), Wang *et al*. (2008) and Hou *et al*. (2009). The DCMD permeate fluxes obtained in this manuscript were up to 5 times higher than the previously obtained in (García-Payo *et al*. 2010). This is due to the higher PEG concentration used. However, these permeate fluxes are up to 8-9 times smaller than those obtained for PVDF hollow fiber membranes developed for DCMD desalination. The reported permeate fluxes were 55 kg/m^{2}h in Bonyadi and Chung (2009), 41.5 kg/m^{2}h in Wang *et al*. (2008) and 40.5 kg/m^{2}h in Hou *et al*. (2009).

Fig. 10 shows the DCMD fluxes of both membranes (PEG3, PEG5) as a function of higher feed temperatures using 30 g/l salt (NaCl) aqueous solution and distilled water as feed. In this case the permeate temperature was maintained constant at 25°C. As it was expected for both membranes, the DCMD flux corresponding to the salt aqueous solution also increased exponentially with the feed temperature and it is lower than that of distilled water used as feed. This is due to the decrease of the vapour pressure with the addition of salt to distilled water.

As observed previously for distilled water used as feed in Fig. 9, the DCMD flux of the hollow fiber membrane PEG5 was also found to be higher than that of the hollow fiber membrane PEG3 when a salt aqueous solution was employed. On the contrary, the salt rejection factor of the hollow fiber membrane PEG5 (97.9%-99.3%) was found to be lower than that of the hollow fiber membrane PEG3 (>99.8%). This decrease of the salt rejection factor may be attributed partially to

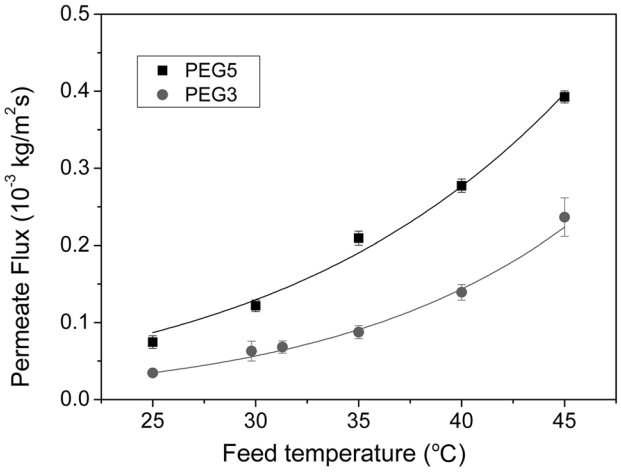

Fig. 9 Effects of PEG concentration and feed temperature on the DCMD permeate flux using distilled water as feed, 20°C permeate temperature. The solid lines represent the best exponential fit of the experimental data

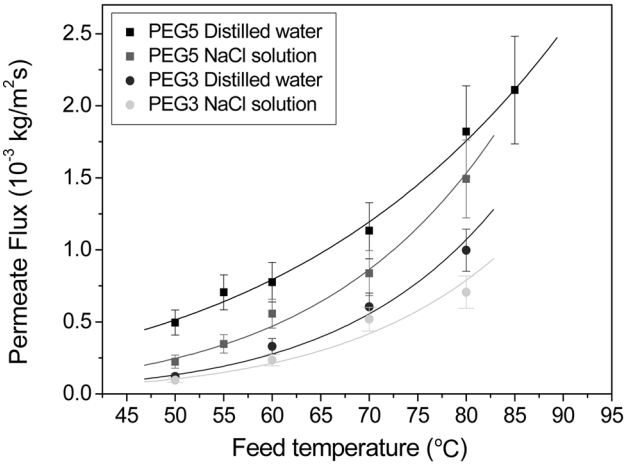

Fig. 10 Effects of the feed temperature on the DCMD permeate flux of the PVDF-HFP hollow fiber membranes prepared with 3 and 5 wt.% of PEG as non-solvent additive, distilled water and 30 g/l aqueous solution were used as feed, 25°C permeate temperature. The solid lines represent the best exponential fit of the experimental data

membrane pore wetting as the inner pore size of the PVDF-HFP hollow fiber membrane PEG5 is larger than that of the hollow fiber membrane PEG3.

4. Conclusions

PVDF-HFP hollow fiber membranes were prepared by the dry/wet spinning technique. It was

observed an increase of the hollow fiber membrane thickness and the void volume fraction with increasing the PEG concentration in the spinning PVDF-HFP solution. Hollow fiber morphology changes have been detected with the variation of the PEG content in the PVDF-HFP spinning solution. The cross-section structure changed from three layers (a middle sponge-type structure between two finger-type structure layers) for the hollow fiber membrane prepared with 5 wt.% in the spinning solution, to two layers (one inner sponge-type structure and one outer finger-type structure) for the hollow fiber membrane spun with 3 wt.%. This structural change was attributed to the increase of the coagulation rate of the copolymer solution with the increase of the PEG concentration in the spinning solution.

The pore size, nodule size and roughness of the internal surface of the PVDF-HFP hollow fiber membranes increased with increasing the PEG concentration. In contrast no clear variation was detected for the pore and nodule size of the outer surfaces.

The DCMD permeate fluxes were greater for the hollow fiber membranes prepared with 5 wt.% PEG concentration, whereas the salt rejection factor was higher for the hollow fiber membrane PEG3, obtaining values higher than 99.8%. The slight diminution of the salt rejection factor observed for the PVDF-HFP hollow fiber membrane PEG5 was attributed to a possible partial wetting of the larger pores of this membrane compared to the pores of the hollow fiber membrane PEG3.

Acknowledgements

The author (M. Essalhi) is thankful to Middle East Desalination Research Centre (MEDRC) for the grant (Project 06-AS007). The authors also gratefully acknowledge the financial support of the Spanish Ministry of Science and Innovation (Project FIS2006-05323). The authors wish also to thank the financial support of the University Complutense of Madrid, UCM-BSCH (Project GR58/08, UCM group 910336).

References

Al-Obaidani, S., Curcio, E., Macedonio, F., Di Profio, G., Al-Hinai, H. and Drioli, E. (2008), "Potential of membrane distillation in seawater desalination: Thermal efficiency, sensitivity study and cost estimation", *J. Membrane Sci*., **323**, 85-98.

Bonyadi, S. and Chung, T.S. (2009), "Highly porous and macrovoid-free PVDF hollow fiber membranes for membrane distillation by a solvent-dope solution co-extrusion approach", *J. Membrane Sci.*, **331**, 66-74.

Cao, J.H., Zhu, B.K. and Xu, Y.Y. (2006), "Structure and ionic conductivity of porous polymer electrolytes based on PVDF-HFP copolymer membranes", *J. Membrane Sci.*, **281**, 446-453.

Chung, T.S.N. (2008), "Fabrication of hollow-fiber membrane by phase inversion", *Advanced Membrane Technology and Applications*, (Eds. Li, N.N., Fane, A.G., Ho, W.S.W. and Matsuura, T.), John Wiley & Sons, New Jersey.

El-Bourawi, M.S., Ding, Z., Ma, R. and Khayet, M. (2006), "A framework for better understanding membrane distillation separation process", *J. Membrane Sci.*, **285**, 4-29.

Feng, C., Wang, R., Shi, B., Li, G. and Wu, Y. (2006), "Factors affecting pore structure and performance of poly(vinylidene fluoride-co-hexafluoropropylene) asymmetric porous membrane", *J. Membrane Sci.*, **277**, 55-64.

García-Payo, M.C., Izquierdo-Gil, M.A. and Fernández-Pineda, C. (2000), "Air gap membrane distillation of aqueous alcohol solutions", *J. Membrane Sci.*, **169**, 61-80.

García-Payo, M.C., Izquierdo-Gil, M.A. and Fernández-Pineda, C. (2002), "Wetting study of hydrophobic membranes via liquid entry pressure measurements with aqueous alcohol solutions", *J. Colloid Interf. Sci.*, **230**, 420-431.

García-Payo, M.C., Rivier, C.A., Marison, I.W. and von Stockar, U. (2002), "Separation of binary mixtures by thermostatic sweeping gas membrane distillation: II. Experimental results with aqueous formic acid solutions", *J. Membrane Sci.*, **198**, 197-210.

García-Payo, M.C., Essalhi, M. and Khayet, M. (2009), "Preparation and characterization of PVDF-HFP copolymer hollow fiber membranes for membrane distillation", *Desalination*, **246**, 96-100.

García-Payo, M.C., Essalhi, M. and Khayet, M. (2010), "Effects of PVDF-HFP concentration on membranes distillation performance and structural morphology of hollow fiber membranes", *J. Membrane Sci.*, **347**, 209-219.

Gryta, M., Tomaszewska, M. and Karakulski, K. (2006), "Wastewater treatment by membrane distillation", *Desalination*, **198**, 67-73.

Hou, D., Wang, J., Qu, D., Luan, Z. and Ren, X. (2009), "Fabrication and characterization of hydrophobic PVDF hollow fiber membranes for desalination through direct contact membrane distillation", *Sep. Purif. Technol.*, **69**, 78-86.

Hwang, Y.J., Jeong, S.K., Nahm, K.S. and Stephan A.M. (2007). "Electrochemical studies on poly(vinylidene fluoride-co-hexafluropropylene) membranes prepared by phase inversion method", *Eur. Polym. J.* **43**, 65-71.

Izquierdo-Gil, M.A., García-Payo, M.C. and Fernández-Pineda, C. (1999), "Direct contact membrane distillation of sugar aqueous solutions", *Sep. Sci. Technol.*, **34,** 1773-1801.

Khayet, M. (2003), "The effects of air gap length on the internal and external morphology of hollow fiber membranes", *Chem. Eng. Sci.*, **58**, 3091-3104.

Khayet, M. (2008), "Membrane distillation", *Advanced Membrane Technology and Applications*, (Eds. Li, N.N., Fane, A.G., Ho, W.S.W. and Matsuura T.), John Wiley & Sons, New Jersey.

Khayet, M. and Matsuura, T. (2001), "Preparation and characterization of polyvinylidene fluoride membranes for membrane distillation", *Ind. Eng. Chem. Res.*, **40**, 5710-5718.

Khayet, M., Feng, C., Khulbe, K.C. and Matsuura, T. (2002), "Preparation and characterization of polyvinylidene fluoride hollow fiber membranes for ultrafiltration", *Polymer*, **43**, 3879-3890.

Khayet, M., Velázquez, A. and Mengual, J.I. (2004), "Direct contact membrane distillation of humic acid solutions", *J. Membrane Sci.*, **240**, 123-128.

Khayet, M., García-Payo, M.C., Qusay, F.A., Khulbe, K.C., Feng, C.Y. and Matsuura, T. (2008), "Effects of gas gap type on structural morphology and performance of hollow fibers", *J. Membrane Sci.*, **311**, 259–269.

Khulbe, K.C., Feng, C.Y., Hamad, F., Matsuura, T. and Khayet, M. (2004), "Structural and performance study of micro porous polyetherimide hollow fiber membranes prepared at different air gap", *J. Membrane Sci.*, **245**, 191-198.

Li, B. and Sirkar, K.K. (2004), "Novel membrane and device for direct contact membrane distillation based desalination process", *Ind. Eng. Chem. Res.*, **43**, 5300-5309.

Li, G.C., Zhang, P., Zhang, H.P., Yang, L.C. and Wu, Y.P. (2008), "A porous polymer electrolyte based on P(VDF-HFP) prepared by simple phase separation process", *Electrochem. Commum.*, **10**, 1883-1885.

Martínez, L. and Rodríguez-Maroto, J.M. (2008), "Membrane thickness reduction effects on direct contact membrane distillation performance", *J. Membrane Sci.*, **312**, 143-156.

Park, H.H., Deshwal, B.R., Kim, I.W. and Lee, H.K. (2008), "Absorption of SO_2 from flue gas using PVDF hollow fiber membranes in a gas–liquid contactor", *J. Membrane Sci.*, **319**, 29-37.

Qtaishat, M., Matsuura, T., Kruczek, B. and Khayet, M. (2008), "Heat and mass transfer analysis in direct contact membrane distillation", *Desalination*, **219**, 272-292.

Qtaishat, M., Rana, D., Khayet, M. and Matsuura, T. (2009), "Preparation and characterization of novel hydrophobic/hydrophilic polyetherimide composite membranes for desalination by direct contact membrane distillation", *J. Membrane Sci.*, **327**, 264-273.

Seol, W.H., Lee, Y.M. and Park, J.K. (2007), "Enhancement of the mechanical properties of PVDF membranes by non-solvent aided morphology control", *J. Power Sources*, **170**, 191-195.

Shi, L., Wang, R., Cao, Y., Feng, C., Liang, D.T. and Tay, J.H. (2007), "Fabrication of poly(vinylidene fluoride-co-hexafluoropropylene) (PVDF-HFP) asymmetric microporous hollow fiber membranes", *J. Membrane Sci.*,

305, 215-225.
Shi, L., Wang, R., Cao, Y., Liang, D.T. and Tay, J.H. (2008), "Effect of additives on the fabrication of poly(vinylidene fluoride-co-hexafluropropylene) (PVDF-HFP) asymmetric microporous hollow fiber membranes", *J. Membrane Sci.*, **315**, 195-204.
Shi, L., Wang, R., Cao, Y. (2009), "Effect of the rheology of poly(vinylidene fluoride-co-hexafluropropylene) (PVDF-HFP) dope solutions on the formation of microporous hollow fibers used as membrane contactors", *J. Membrane Sci.*, **344**, 112-122.
Song, L., Li, B., Sirkar, K.K. and Gilron, J.L. (2007), "Direct contact membrane distillation-based desalination: novel membranes, devices, larger-scale studies and a model", *Ind. Eng. Chem. Res.*, **46**, 2307-2323.
Stephan, A.M., Renganathan, N.G., Gopukumar, S. and Teeters, D. (2004), "Cycling behavior of poly(vinylidene fluoride-co-hexafluoro propylene) (PVDF-HFP) membranes prepared by phase inversion method", *Mater. Chem. Phys.*, **85**, 6-11.
Teoh, M.M., Bonyadi, S. and Chung, T.S. (2008), "Investigation of different hollow fiber module designs for flux enhancement in the membrane distillation process", *J. Membrane Sci.*, **311**, 371-379.
Tian, X. and Jiang, X. (2008), "Poly(vinylidene fluoride-co-hexafluoropropylene) (PVDF-HFP) membranes for ethyl acetate removal from water", *J. Hazard. Mater.*, **153**, 128-135.
Tomaszewska, M. (1996), "Preparation and properties of flat-sheet membranes from poly(vinylidene) fluoride for membrane distillation", *Desalination*, **104**, 1-11.
Wang, D., Li, K. and Teo, W.K. (1999), "Preparation and characterization of polyvinylidene fluoride (PVDF) hollow fiber membranes", *J. Membrane Sci.*, **163**, 211-220.
Wang, K.Y., Chung, T.S. and Gryta, M. (2008), "Hydrophobic PVDF hollow fiber membranes with narrow pore size distribution and ultra-thin skin for the freshwater production through membrane distillation", *Chem. Eng. Sci*,. **63**, 2587-2596.
Yeow, M.L., Liu, Y.T. and Li, K. (2004), "Morphological studies of poly(vinylidene fluoride) asymmetric membranes: effect of the solvent, additive and dope temperature", *J. Appl. Polym. Sci.*, **92**, 1782-1789.
Zhang, M., Zhang, A.Q., Zhu, B.K., Du, C.H. and Xu, Y.Y. (2008), "Polymorphism in porous poly(vinylidene fluoride) membranes formed via immersion precipitation process", J. *Membrane Sci.*, **319**, 169-175.

CC